Int. J. Electrochem. Sci., 16 **(2021)** Article ID: 210934, doi: 10.20964/2021.09.27

International Journal of
ELECTROCHEMICAL
SCIENCE
www.electrochemsci.org

Short Communication

Effect of H_2 Flow Rate on Corrosion Resistance of Tantalum Coating Prepared on Molybdenum via Chemical Vapor Deposition

HaiJun Wu[1,4]*, Jingchang Chen*[2]*, Xu Xing*[2]*, Hongzhong Cai*[4]*, Hua Li*[3,*]*, Xiao Wang*[1,3*]*,*

[1] School of Materials Science and Engineering, Kunming University of Science and Technology, Kunming, 650093, China;
[2] School of Machinery and Communications, Southwest Forestry University, Kunming, 650224, China;
[3] City college, Kunming University of Science and Technology, Kunming, 650093, China;
[4] Kunming Institute of Precious Metals, Kunming, 650106, China.
[*]E-mail: whj@ipm.com.cn, w_ang_xiao@sina.com

Received: 16 April 2021 / *Accepted:* 10 June 2021 / *Published:* 10 August 2021

Tantalum coatings prepared via chemical vapor deposition (CVD) tantalum are a key material for service in extremely corrosive environments, and are especially important in the aerospace, weapon equipment, and nuclear industries. However, a strong preferred orientation, which affects the corrosion resistance of the coatings, typically develops during the deposition process of these coatings. In this work, the effects of hydrogen gas (H_2) flow rate on the preferred orientation of a tantalum coating were investigated via first-principles calculations and experiments. The effects on the surface energy and work function of different crystal planes and the corrosion resistance of the coatings were also investigated. The results revealed that the lowest texture coefficient and weakest preferred orientation occur for the coating prepared at 400 mL/min. Similarly, the (110) crystal plane of tantalum had lower surface energy (0.145 eV) and higher work function (4.742 eV), and exhibited better corrosion resistance than the other planes. More importantly, the corrosion potential and the corrosion current density of the coating prepared with 400 mL/min H_2 flow were -0.424 V and 0.535 $\mu A\cdot cm^{-2}$, respectively, and this coating exhibited the highest corrosion resistance. The present work can serve as a reference for improving the corrosion resistance of tantalum coatings.

Keywords: tantalum coating; corrosion resistance; H_2 flow rate

1. INTRODUCTION

With the development of aerospace technologies, weapon equipment, and nuclear industry, the demand for new materials suitable for extreme environments (strong oxidation, strong corrosion, and

ultra-high temperatures) has increased [1–3]. Due to its unique physico-chemical properties, tantalum has become one of the key corrosion-resistant materials [4, 5]. The stability and service life of tantalum coatings are, however, affected by anisotropic corrosion, which can lead to catastrophic accidents involving tantalum serving in a strong corrosive medium [6]. With the aim of resolving these problems, the anisotropic corrosion of tantalum has received considerable attention in recent years [7, 8].

Many studies have shown that anodic oxidation, process parameter adjustment, surface modification technique, and activation are effective in improving the selective corrosion of materials [9–11]. Anodic oxidation and tuning of the process parameters are simpler, more convenient, and more widely used than the other methods. For example, Wilcox et al. [12] showed that anodic oxidation is beneficial for increasing the thickness and uniformity of tantalum coatings, and improving the corrosion resistance of the coatings. Balla et al. [13] reported that adjustment of the deposition temperature is effective in improving the characteristics and corrosion resistance of tantalum coatings. Many studies have shown that the anisotropic corrosion principle and improvement mechanism can be revealed through theoretical simulations [14, 15]. Yao et al. [16] simulated (via first-principles calculations) the anti-oxidation and corrosion behavior of graphene in a seawater environment. Similarly, Gao et al. [17] studied (by means of first-principles calculations) the corrosion resistance of Nb, Sn, Cu, Fe, and Cr on the Zr (0001) crystal plane. However, only a few reports have focused on predicting the corrosion resistance of tantalum via theoretical calculations, and investigations considering the regulatory mechanisms are rare. Clarification of the mechanism governing the relationship between the preferred orientation and corrosion resistance of tantalum coatings is essential for realizing further improvements in the resistance of these coatings.

We found from a previous study that the preferred orientation of the crystalline grains comprising a CVD tantalum coating can be improved by adjusting the deposition parameters. However, the mechanism governing corrosion resistance of the coating remains unclear. In this work, the effect of H_2 flow rate on the preferred orientation and corrosion resistance of a tantalum coating is investigated. The relationship between this orientation and the resistance is established via first-principles calculations and experiments. Through this approach, the mechanisms governing selective corrosion are clarified.

2. EXPERIMENTAL AND COMPUTATIONAL DETAILS

2.1 Preparation of CVD tantalum films

A tantalum coating was prepared by means of chemical vapor deposition (CVD) performed using a vertical tube reactor. The raw materials were a tantalum plate (≥99.99 wt.%) and a molybdenum plate (60 mm × 40 mm × 30 mm). Chorine gas (Cl_2) and hydrogen gas (H_2) each with a purity of >99.9% were used as the oxidizing gas and reducing gas, respectively. The chlorination chamber and the surface treatment substrate were heated using an electric furnace and intermediate frequency induction furnace, respectively. During the deposition process (flow rate of Cl_2: 50–200

mL/min), the pressure of the deposition chamber was maintained at ~105 Pa. Furthermore, H_2 flow rates of 400 mL/min, 600 mL/min, and 800 mL/min were employed. The total thickness of the tantalum coating is ~2 mm. The substrate (Mo plate) and the deposited material (Ta coating; see Fig.1 for a schematic of the coating) were separated by wire cutting and chemical etching.

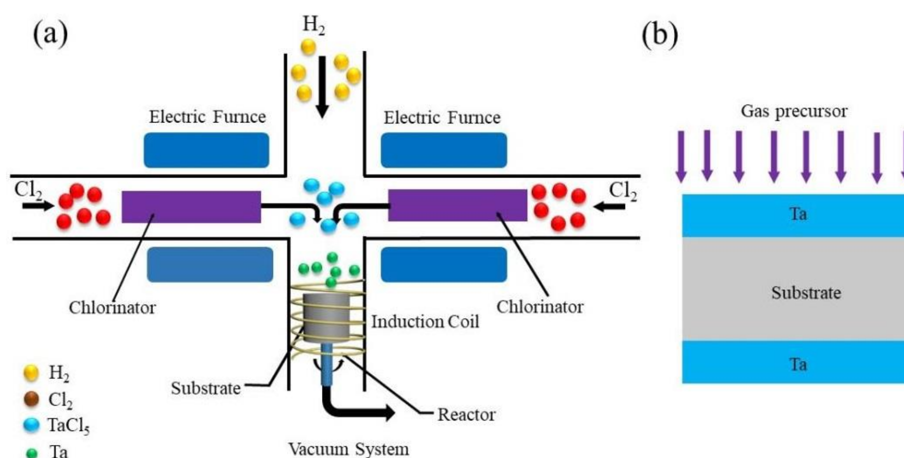

Figure 1. Schematic of tantalum coating prepared via chemical vapor deposition (CVD) (a) and structure of the coating (b).

The main reactions that occur during the CVD process are as follows:

$$2Ta + 5Cl_2(g) \rightarrow 2TaCl_5 \quad (1)$$

$$2TaCl_5 + 5H_2(g) \rightarrow 2Ta + 10HCl(\mathrm{g}) \quad (2)$$

2.2 Materials Characterization and Electrochemical Measurements

The surface morphology of tantalum coatings prepared with different H_2 flow rates were observed via scanning electron microscopy (SEM; XL-30Philips, Japan). Meanwhile, the crystalline structure of the coatings was characterized by means of X-ray diffraction (XRD; D/MAX-RC Japan) using a Cu-Kα radiation source. A tube flow of 200 mA, a tube pressure of 40 kV, a scanning speed of 1°/min, and 10–90° coupled continuous scanning with steps of 0.02° were employed during data collection.

The electrochemical measurements were performed using a CH604E electrochemical workstation (CH Instruments, Shanghai, People's Republic of China). A 99.99% platinum electrode, 10 mm × 10 mm × 2 mm tantalum coating, and saturated calomel electrode were used as the counter electrode, working electrode, and counter electrode, respectively. Tests were performed in an open system at a temperature of 25 ± 0.1 °C with a 3.5% NaCl solution as the electrolyte. Furthermore, the potentiodynamic curves were recorded from -0.3 V to 0.3 V (scanning rate: 0.5 mV/s) at 25 °C. The corrosion potential (E_{corr}) and corrosion current density (I_{corr}) were determined using the Tafel extrapolation method.

2.3 First-principles calculation

First-principles calculations were performed via the Vienna Ab initio Simulation Package (VASP) with periodic boundary conditions using the projector augmented wave (PAW) approach. Based on the surface texture analysis, a seven layer plane of low-index facets including the (110), (200), and (211) planes was established. A 15 Å vacuum space between sheets was set to avoid the periodic effect. The work function calculations were described by Perdew-Burke-Ernzerhof (PBE) generalized gradient approximation (GGA), and Electronic exchange-correlation effects were instituted with local density approximation (LDA) for surface energy calculations. A Brillouin zone with a Monkhorst-Package scheme was used for sampling during structure optimizations and a k-point grid of 7×7×1 was employed. Moreover, the cutoff energy for the plane-wave basis was set to 500 eV. For ionic relaxations, the convergence criterion of our self-consistent calculations was 10^{-6} eV, and the atomic forces were <0.01 eV/Å.

3. RESULTS AND DISCUSSION

3.1 Surface morphology and element composition of the tantalum coating

The hydrogen flow rate, which is an important parameter for the deposition process, can affect the surface morphology and properties of the tantalum coating. Figure 2 shows the surface morphology of coatings prepared with different H_2 flow rates and a constant deposition temperature and Cl_2 flow rate. As shown in the figure, these conditions yield a pyramidal-shape for the morphology of the coatings. Moreover, we also find that the deposition rate of tantalum increases with increasing H_2 flow rate. The size and height of the pyramid-like structure increase correspondingly, leading to a reduction in the surface flatness and uniformity of the coating.

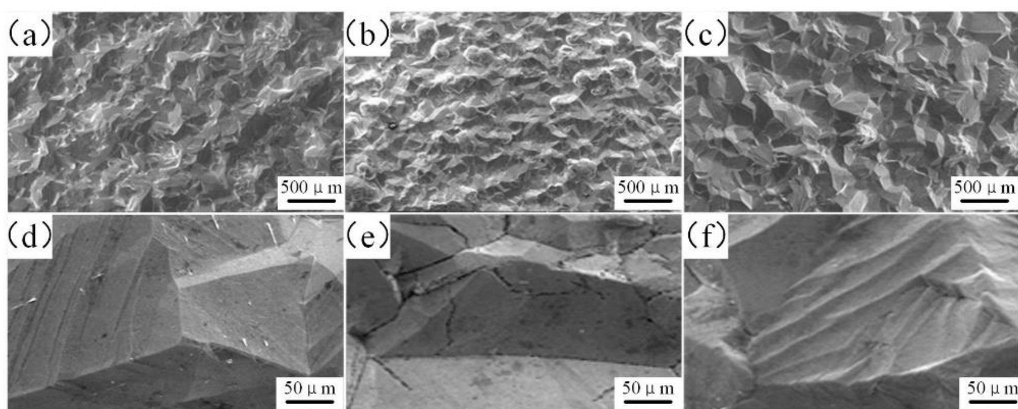

Figure 2. Surface morphologies of coatings prepared with different H_2 flow rates (a, d) 400 mL/min (b, e) 600 mL/min (c, f) 800 mL/min.

The effect of H_2 flow rate on the phase composition of the tantalum coating is analyzed via XRD measurements of coatings prepared with different flow rates (see Fig. 3). As shown in the figure, the diffraction peaks of the coatings concur with the standard PDF card (JSPDS 08-0385), indicating that the tantalum coating is mainly composed of α-Ta with a body-centered cubic structure. However, the detection of tantalum oxide is impossible, due to the small amount of the oxide, which is mainly distributed on the surface of the coating, thereby preventing detection via XRD. We also observe that the diffraction peak intensity of different crystal planes varies with the H_2 flow rate. This may have resulted from the fact that the reaction gas flow rate has an effect on the preferred orientation of the tantalum coating grains. Tantalum and oxygen are strongly bound. Nevertheless, no tantalum oxide is detected in the coating, owing possibly to the aforementioned factors.

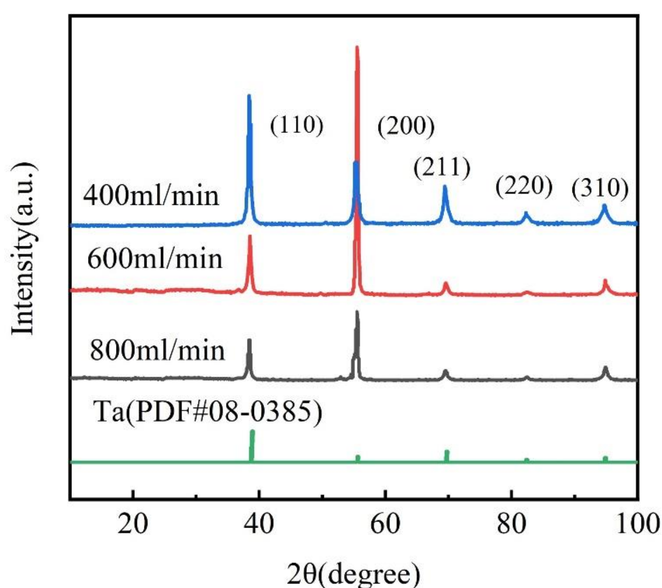

Figure 3. XRD spectra of coatings prepared with different H_2 flow rates; test parameters: Cu-Kα radiation, tube flow: 200 mA, tube pressure: 40 kV, scanning speed: 1°/min, and scan range: 10–90° (coupled continuous scanning with steps of 0.02°).

3.2 Texture coefficient of the coatings prepared with different H_2 flow rates

The preferred orientation of a crystal grain, which is generally expressed in terms of the texture coefficient (T_c), has considerable influence on the corrosion resistance of metallic materials. The coefficient can be calculated from formula (3). If all diffraction planes have the same T_c value, the orientation of the crystal planes is disordered. If the T_c value of a (hkl) crystal plane is greater than the average value, the crystal plane is the preferred orientation, and the T_c value increases with increasing intensity of the orientation [18].

$$T_c(hkl) = \frac{I_{(hkl)}/I_{0(hkl)}}{\sum_N I_{(hkl)}/I_{0(hkl)}} \tag{3}$$

Where, $I_{(hkl)}$ and $I_{0(hkl)}$ are the intensity of the diffraction peak associated with crystal face (hkl), respectively. Similarly, N denotes the number of diffraction peaks.

The texture coefficients of coatings with different H_2 flow rates are shown in Fig. 4. As shown in the figure, the coefficients of the coatings change with increasing flow rate, and the preferred orientation of the tantalum coating varies with the flow rate. When the flow rate of H_2 is 400 mL/min, the largest texture coefficient is obtained for the (110) crystal plane, indicating that the flow rate promotes the preferential growth of the coating on this plane. Similarly, a flow rate of 600 mL/min promotes the growth of the tantalum coating on the (200) crystal plane. This may have resulted from the fact that the H_2 flow rate affects the growth process of the coating grains, thereby changing the preferred orientation of the grains. As established by VAN DER DRIFT'S model, the coating deposition process involves grain nucleation, competitive growth, and engulfment processes [19]. With increasing deposition time, increasing numbers of grains are engulfed by adjacent grains, and the grains in the fastest growing direction dominate the process, leading to the formation of texture.

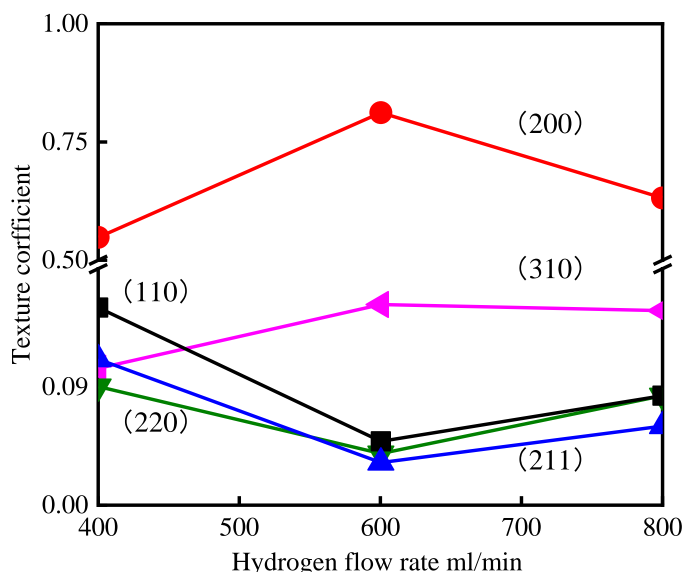

Figure 4. Texture coefficients of coatings with different H_2 flow rates; test parameters: Cu-Kα radiation, tube flow: 200 mA, tube pressure: 40 kV, scanning speed: 1°/min, and scan range: 10–90° (coupled continuous scanning with steps of 0.02°).

3.3 Surface energy of tantalum coating with different crystal planes

The surface energy, which is defined as the work required per unit area to form a new surface, can be calculated as follows [20]:

$$\gamma = (E_{slab} - N \cdot E_{bulk})/2A \qquad (4)$$

Where, E_{slab} is the total energy of the slab, E_{bulk} is the bulk energy obtained for the bulk divided by the number of atoms used in the calculation, N is the number of atoms in the slab, and A is

the surface area. High surface energy can lead to destabilized states, and the stability of a state increases with decreasing surface energy.

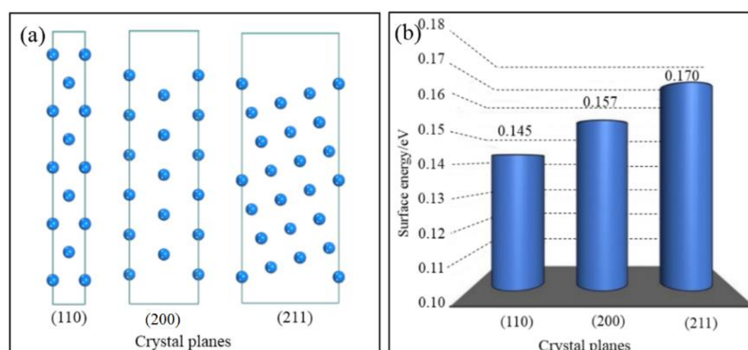

Figure 5. Surface energies of different crystal planes ((110), (200), and (211)). (a) Model of each crystal plane and (b) surface energy of (as calculated by VASP) each plane.

The surface energy (γ) of crystalline materials has a significant effect on the corrosion resistance. That is, a high surface energy indicates that the density of atoms is large, the inter-atomic distance is small, the bonding force of atoms is large, and the surface is easily corroded. To determine the corrosion resistance of the tantalum coating from the surface energy of a crystal plane, the energy of different planes is calculated using the VASP package based on density functional theory (see Fig. 5). Surface energies of 145 eV, 0.157 eV, and 0.169 eV are obtained for the (110), (200), and (211)) planes, respectively. Therefore, $\gamma_{(211)} > \gamma_{(200)} > \gamma_{(110)}$, indicating that, of the three planes considered, the (110) crystal plane is the least prone to chemical reactions.

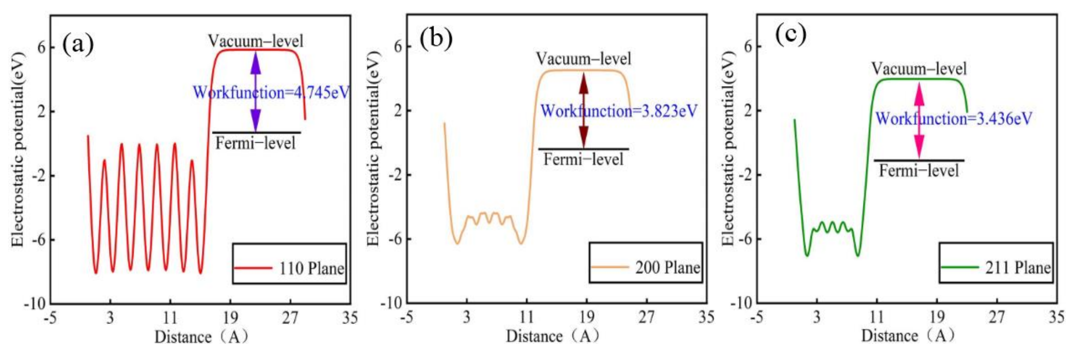

Figure 6. Work functions (as calculated by VASP) of different crystal planes (a) (110); (b) (200); (c) (211).

To determine the propensity for chemical reactions on crystal planes, we calculate the work functions of different crystal planes ((110), (200), and (211); see Fig. 6). The work function, which is the energy required for an electron to transfer from the Fermi level to the vacuum potential, is calculated as follows [21]:

$$\emptyset = E_{vac} - E_f \quad (5)$$

Where, E_{vac} is the electrostatic potential in the vacuum near the surface, and E_f is the Fermi level (electrochemical potential of electrons) inside the material.

From the figure, the surface work function values of the (110), (200), and (211) crystal plane are 4.742 eV, 3.827 eV, and 3.435 eV, respectively. High surface work function values indicate that the surfaces may suppress the chemical reactions [22]. The work function of (110) crystal plane is the largest, indicating that corrosion of the (110) crystal plane of tantalum is difficult. From the above analysis, this crystal plane has lower surface energy and higher work function than the (200) and (211) planes, and exhibits the best corrosion resistance. When a H_2 flow rate of 400 mL/min is employed, the largest texture coefficient is obtained for the (110) crystal plane, indicating that the flow rate promotes preferential growth of the coating on this crystal plane. Therefore, the corrosion resistance of the tantalum coating can be improved by controlling the growth of tantalum on the (110) crystal plane.

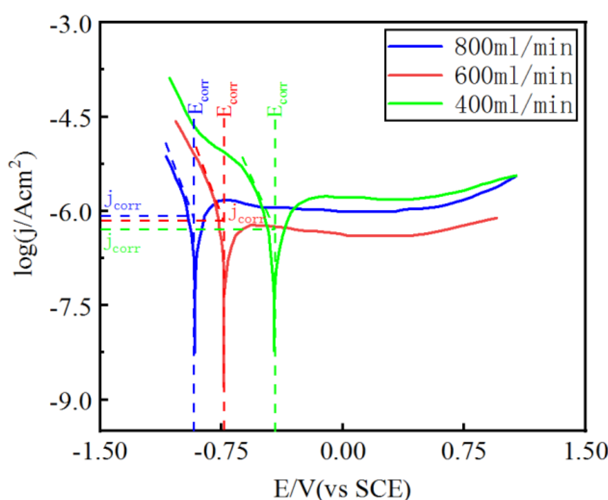

Figure 7. Potentiodynamic polarization curves of the samples prepared with different H_2 flow rates in 3.5 wt.% NaCl solution at 25 °C.

In order to verify the results of the first-principles calculation, the electrochemical performance of the coatings is determined using a typical three-electrode electrochemical workstation in a 3.5 wt.% NaCl solution at 25 °C (see Fig.7 and Table 1). As shown in the figure, the corrosion potential (E_{corr}) of the coatings prepared at H_2 flow rates of 400 mL/min, 600 mL/min, and 800 mL/min are approximately −0.424 V, −0.740 V, and −0.918 V, respectively. The corresponding corrosion current density (j_{corr}) values of the coating are approximately 0.535 μA/cm^2, 0.742 μA/cm^2, and 0.832 μA/cm^2, respectively. The results show that the E_{corr} and j_{corr} of the coating prepared at 400 mL/min are higher and lower, respectively, than those of the other samples. Therefore, this sample exhibits the best corrosion resistance. Compared with other processing methods, adjustment of the hydrogen flow rate yields a considerably greater improvement in the corrosion resistance of the tantalum coating [23]. This results mainly from the fact that the (110) crystal planes occur with weak intensity in the coating

prepared with 400 mL/min H_2 flow. This weak intensity is beneficial for improving the corrosion resistance of the coating.

Table 1. Corrosion parameters of the samples prepared at different H_2 flow rates in 3.5 wt.% NaCl solution at 25 °C.

H_2 flow rates	E_{corr}/V_{SCE}	$j_{corr}/\mu A.cm^{-2}$	β_c/ $mV.dec^{-1}$	β_a/ $mV.dec^{-1}$
400 ml/min	-0.424	0.535	155	-96.4
600 ml/min	-0.740	0.742	125	-95.6
800 ml/min	-0.918	0.832	116	-94.6
Tantalum[23]	-0.66	1.1	-	-

4. CONCLUSIONS

In this work, the effect of H_2 flow rate on the corrosion resistance of a tantalum coating is investigated. The results revealed that the texture coefficients of each coating change with increasing H_2 flow rate. The lowest texture coefficient and weakest preferred orientation are obtained for the coating prepared at a flow rate of 400 mL/min. Furthermore, compared with the (200) and (211) crystal planes, the (110) crystal plane of tantalum has lower surface energy (0.145 eV) and higher work function (4.742 eV), and exhibits better corrosion resistance. More importantly, the corrosion potential (E_{corr}) and the corrosion current density (j_{corr}) of the coating prepared at a H_2 flow rate of 400 mL/min are −0.424 V and 0.535 $\mu A \cdot cm^{-2}$, respectively. This coating exhibits the best corrosion resistance. The above analysis indicates that the H_2 flow rate has a significant effect on the preferred orientation and hence the corrosion resistance of the CVD coating. Therefore, the corrosion resistance of the coating can be improved by adjusting the H_2 flow rate. This work can serve as a reference for improving the corrosion resistance of tantalum coatings prepared via CVD.

ACKNOWLEDGEMENTS
This work was supported financially by the Scientific Research Fund of Yunnan Education Department (grant Nos. 2020J0416 and 2019J0039); the National Nature Science Foundation of China (grant Nos. 52061019); Key projects of basic research plan of Yunnan Science and Technology Department (grant Nos. 202001AS070048). General projects of basic research plan of Yunnan Science and Technology Department (grant Nos. 202001AT070147).

References

1. X.S. Zhang, Y.J. Chen and J.L. Hu, *Prog. Aerosp. Sci*., 97 (2018) 22.
2. P. Lu, J.E. Saal, G.B. Olson, T. Li, O.J. Swanson and J.R. Scully, *Scripta. Materialia*., 153 (2018) 19.
3. J.C. Zhao and J.H. Westbrook, *MRS. bulletin*., 28 (2003) 622.
4. Y.L. Zhou, M. Niinomi, T. Akahori, M. Nakai and H. Fukui, *Metall. Mater. Trans. B*., 48 (2007) 380.

5. T.Y. Kuo, W.H. Chin, C.S. Chien and Y.H. Hsieh, *Surf. Coat. Technol*., 372 (2019) 399.
6. S.M. Cardonne, P. Kumar, C.A. Michaluk and H.D. Schwartz, *Int. J. Refract. Met. H*., 13 (1995) 187.
7. A. Robin and J. Rosa, *Int. J. Refract. Met. Hard Mater*., 18 (2000) 13.
8. D.L. Zhao, C.J. Han, L. Yan, J.J. Li, K. Zhou, Q.S. Wei, J. Liu and Y.S. Shi, *J. Alloys Compd*., 804 (2019) 288.
9. Q. Chao, V. Cruz, S. Thomas, N. Birbilis, P. Collins, A. Taylor, P.D. Hodgson and D. Fabijanic, *Scripta Mater*., 141 (2017) 94.
10. J. Suryawanshi, T. Baskaran, O. Prakash and S.B. Arya, *Mater*., 3 (2018) 153.
11. Y. Chen, J.X. Zhang, N.W. Dai, Q. Qin, H. Attar and L.C. Zhang, *Electrochim. Acta.*, 232 (2017) 89.
12. P.S. Wilcox and W.D. Westwood, *Can. J. Phys*., 49 (1971) 1543.
13. V.K. Balla, S. Banerjee, S. Bose and A. Bandyopadhyay, *Acta. Biomater*., 6 (2010)
14. 2329.
15. Y. Lu, S. Luo, Z. Ren, Y. Zou and M. Yang, *Surf. Coat. Technol*., 409 (2021) 126833.
16. C.D. Taylor, M. Neurock and J.R. Scully, *J. Scully, J. Electrochem. Soc*., 155 (2008) C407.
17. W.J. Yao, S.G. Zhou, Z.X. Wang, Z.B. Lu and C.J. Hou, *Appl. Surf. Sci*., 499 (2020) 143962.
18. H. Gao, Z.F. Yang, J.H. Zhao, H.M. Yuan, Z.E. Zhao and X. Zhao, *J.Comput.Phys*.,7 (2021) 5.
19. S.L. Lee, M. Doxbeck, J. Mueller and P. Cote, *Surf. Coat. Technol*., 177 (2004) 44.
20. T.D. Manning, I.P. Parkin and M.E. Pemble, D. Sheel and D. Vernardou, *Chem. Mater*., 16 (2004) 744.
21. Y.B. Zhang, D.A. Kitchaev, J.L. Yang, T.N. Chen and J.W. Sun, *NPJ. Comput. Mater*., 4 (2018) 1.
22. V.V. Zhirnov, S. Pandey and G. Sandhu, *Mater. Res. Express*., 5 (2018) 056308.
23. H. Lin, J.X. Liu, H.J. Fan and W.X. Li, *J. Phys. Chem. C. Nanomater. Interfaces*., 124 (2020) 11005.
24. H. Koivuluoto, J. Näkki and P. Vuoristo, *J. Therm. Spray. Techn*., 18 (2009) 75.

© 2021 The Authors. Published by ESG (www.electrochemsci.org). This article is an open access article distributed under the terms and conditions of the Creative Commons Attribution license (http://creativecommons.org/licenses/by/4.0/).